Journal of Electroceramics 4:2/3, 319–325, 2000


# Effect of Ultra-Thin $SrTiO_3$ Seed Layer on the Microwave Surface Resistance of $YBa_2Cu_3O_7$ Films Deposited on (1 0 0) MgO

C. COUVERT,[1] J.P. CONTOUR,[1] O. DURAND,[2] Y. LEMAÎTRE,[1] B. MARCILHAC[1] & P. WOODALL[1]
[1]*Unité Mixte de Physique C.N.R.S./Thomson-CSF, F-91404 Orsay, France*
[2]*LCR/Thomson-CSF, F-91404 Orsay, France*

**Abstract.** RHEED controlled ultra-thin buffer layers of $SrTiO_3$ have been deposited on (1 0 0) MgO by pulsed laser deposition to grow $YBa_2Cu_3O_7$ films for microwave applications. A buffer layer with a thickness from 5 to 40 unit cells of $SrTiO_3$ is sufficient to expand to more than 60°C the range of deposition temperatures for which a low microwave surface resistance [Rs(10 GHz, 77 K) < 0.5 mΩ] is obtained. The Rs values are as low as those obtained on $LaAlO_3$ substrates, furthermore they present a slightly lower magnetic field dependency. The XRD Φ-scans show that the $SrTiO_3$ seed layer induces an oriented epitaxial growth with the [1 0 0] axis of YBCO parallel to the one of MgO over this broadened range of deposition temperatures. This seed layer promoting effect is not observed with other oxides such as $Ba_{0.15}Sr_{0.85}TiO_3$, $CeO_2$, $Ce_{1-x}La_xO_2$.

**Keywords:** high temperature super conductors, microwave properties, thin films, pulsed laser deposition

## 1. Introduction

Magnesium oxide with its high crystalline quality and low dielectric loss ($0.4 \times 10^{-6}$at 77 K) would be a perfect substrate for microwave applications of HTSC, however few high quality results have been reported using these substrates due to the poor reproducibility in Rs and the drastic dependance of Rs on the growth parameters, especially on the substrate temperature [1–5]. In a previous paper we have shown that $YBa_2Cu_3O_7$ (YBCO) films grown on MgO substrates with Rs values lower than 0.5 mΩ (77 K, 10 GHz) were obtained within an extremly narrow temperature range [6]. It was also observed that the lowest Rs values were found to be correlated with the lowest RBS yield in channeling geometry and with the lowest quantity of misaligned *c*-axis grains. At the same time it has been reported first by Prouteau *et al*. that a 25 nm thick buffer layer of $SrTiO_3$ deposited on MgO improves markedly the superconductive properties of the subsequently deposited YBCO layer [7] and then by Cui *et al*. that a $SrTiO_3$ buffer layer as thin as 6 nm is sufficient to grow highly crystalline YBCO thin films on MgO substrates [8]. The influence of the microstructure of a 20 nm thick $SrTiO_3$ buffer layer on the microwave properties of the YBCO film was studied by M.R. Rao who reported that the microwave loss in YBCO was correlated to the $SrTiO_3$ grain size [9]. Finally, we recently reported that an ultra-thin $SrTiO_3$ buffer layer increases markedly the deposition temperature range in which low Rs values are obtained [10]. In this paper we report on the effect of an ultra-thin oxide seed layer deposited on MgO substrates on the electrical and microwave properties of the subsequently deposited YBCO film and try to explain the drastic effect of $SrTiO_3$ with respect to some other oxides such as $Ba_{0.15}Sr_{0.85}TiO_3$, $CeO_2$, $Ce_{1-x}La_xO_2$.

## 2. Experimental

Films were prepared *in situ* by PLD in a multitarget LDM 32 Riber machine using a frequency tripled Nd:YAG laser (B.M. Industries 503 DNS) which delivers a laser beam of 355 nm wavelength with a power density of 600 MW/cm$^2$ after focussing the laser beam on the target. The deposition rate is

0.22 nm/s for $SrTiO_3$ and 0.26 nm/s for YBCO at a repetition rate of 2.5 Hz and a substrate-target distance of 33 mm. The $Ba_{0.15}Sr_{0.85}TiO_3$, $CeO_2$, $Ce_{1-x}La_xO_2$ and YBCO targets are stoechiometric sintered disks with a density higher than 0.9 of the theoretical one, and the $SrTiO_3$ target is cut from a monocristalline rod; they are continuously moved to ensure a uniform ablation rate. Before the growth the (1 0 0) MgO substrates are cleaned by heating in pure oxygen up to 800°C for 10 min at a pressure of 40 Pa. After this cleaning procedure, cleanliness and flatness of the surface are verified by RHEED before starting the growth procedure. The substrate temperature is maintained at 700°C and the pressure around $10^{-4}$ Pa during the $SrTiO_3$ deposition so that the RHEED patterns can be continuously recorded during the growth by using a differentialy pumped electron gun (EK-35 Staib Instrumente GmbH). On the other hand, the YBCO layers of cuprate heterostructures are grown at 780°C under 40 Pa of molecular oxygen, a high value required for the growth of HTc oxides; consequently the RHEED patterns are only recorded at the end of the process after further oxygen pumping [10].

The surface resistance (Rs) measurements were carried out at 77 K and 10 GHz by the dielectric resonator method using titanium oxide ($TiO_2$) as a dielectric. The diameter and the thickness of the resonator are 7 and 1 mm respectively, its dielectric constant is 105 with a loss coefficient of $1 \times 10^{-5}$ at 77 K [11,12]. The Rs values are measured on 400 nm thick YBCO films and are given without any thickness correction.

XRD analysis has been carried out by using $\theta/2\theta$ and 4-circle X-ray diffractometers in Bragg-Brentano-geometry with CuK$\alpha$ sources.

## 3. Results and Discussion

Figure 1 presents the diffraction patterns recorded as a function of time during the first stage of the $SrTiO_3$ growth on MgO. The growth starts in a 3D mode which is clearly evidenced by the spotty pattern observed immediately after the impinging of the first species at the substrate surface. However, a streaky $SrTiO_3$ diffraction pattern is recovered after the deposition of about 4 elementary cells. This 2D mechanism induces weak RHEED intensity oscillations which are detected from about 12 $SrTiO_3$ cells but which are markedly weaker than those recorded during the homoepitaxial growth of $SrTiO_3$ [10,13]. At the same time, the in-plane parameter changes sharply from 0.428 nm to 0.396 nm during the deposition of the 6 first cells, after that it decreases slowly to 0.392 nm during the deposition of the next 10 cells and stabilizes about this value (Fig. 2). The limit of elastic accomodation of $SrTiO_3$ on MgO with a critical thickness of 2.5 nm which is deduced from this measurements is in good agreement with our previous calculations performed using an energy based model [14].

Taking into account the high mismatch of the system ($\Delta a/a = 7.2\%$) the appearance of a streaky RHEED pattern after the deposition of a few unit cells of $SrTiO_3$ is surprising, because a markedly spotty pattern is observed after the deposition of an equivalent thickness for most of the other oxides that we try to deposit on MgO. For example, in the case of $Ce_{0.69}La_{0.31}O_{1.845}$ ($a = 0.388$ nm), the RHEED pattern evidences clearly a streaky plot associated with a 2D growth mechanism on $SrTiO_3$ ($\Delta a/a = 0.6\%$) but a spotty one on MgO ($\Delta a/a = 7.8\%$) which is highly mismatched to the epilayer (Fig.3).

The AFM roughnesses determined over 5 $\mu$m after the deposition of 6, 12, 24 and 36 unit cells of $SrTiO_3$ which are summarized in Fig. 4 are in good agreement with the RHEED observations : the flatness of the surface is optimized with a buffer layer thickness up to 24 elementary cells, the 12 cell seed layer used in this study being in the middle of the roughness plateau.

We tried then to determine the range of deposition temperature leading to the lowest Rs value of the YBCO layer deposited on $SrTiO_3$ buffered MgO and to confirm the optimized thickness of the seed layer which was deduced from the RHEED analysis. The surface resistances of 400 nm thick YBCO films as a function of the substrate temperature are plotted in Fig. 5. Two significant differences are observed with respect to our previously reported results on MgO substrates [11]. First, the substrate temperature range in which the surface resistance is lower than 0.5 m$\Omega$ becomes far broader with $SrTiO_3$ buffered MgO ($\Delta Ts \simeq 65$°C) than with bare MgO ($\Delta Ts \leq 10$°C) and then the deposition temperatures are shifted upwards of around 30°C, consequently the deposition conditions become close to those of $LaAlO_3$ substrates.

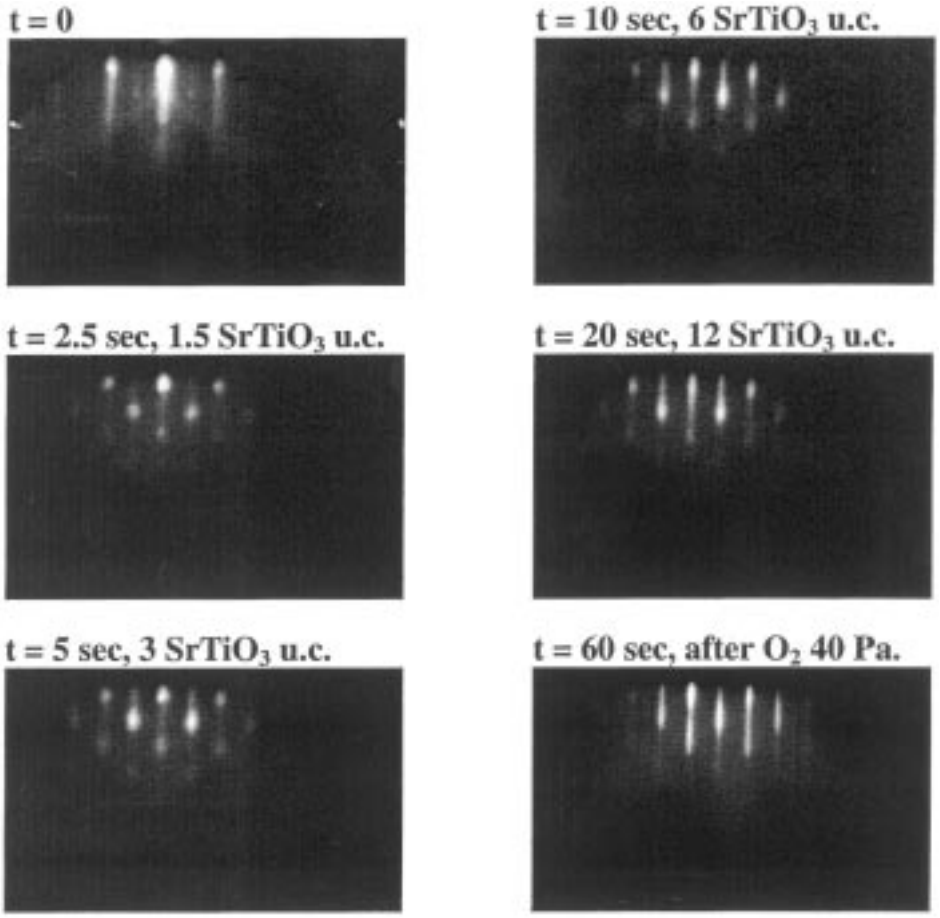


*Fig. 1.* RHEED patterns recorded along the (1 0 0) azimuth of the MgO substrate as a functions of the time of deposition of the $SrTiO_3$ seed layer.

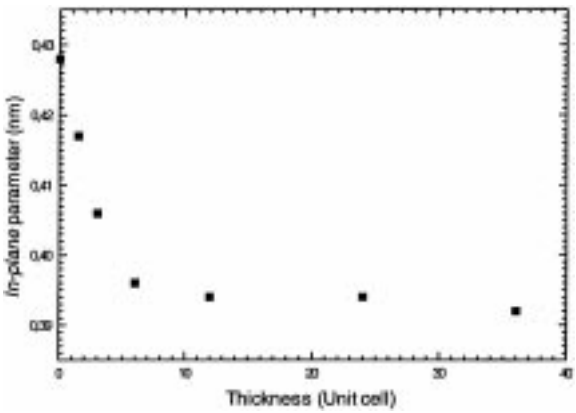


*Fig. 2.* Variation of the in-plane parameter determined from the RHEED measurements versus the thickness of the buffer layer in elementary unit cell of $SrTiO_3$, i.e., 0.39 nm.

The broadening of the range of growth temperature is of paramount importance for the deposition over large area substrate for which the temperature uniformity is never perfect and also for double-sided deposition. The surface resistance of the subsequently deposited YBCO film has then been studied as a function of the thickness of the $SrTiO_3$ seed layer. The plot in Fig. 6 confirms that the thickness which is set based on the RHEED analysis is close to the optimized value, Rs increases gently with increasing microwave power up to a field of 10 Oe, the slope (i.e., the power dependency) being $1.6 \times 10^{-3}$ m$\Omega$/Oe whereas it is $9.5 \times 10^{-3}$ m$\Omega$/Oe for the YBCO layers grown on $LaAlO_3$ in our PLD system. The results which are summarized in Table 1 show that no other ultra-thin

*Table 1.* Microwave properties of a 400 nm thick YBCO layer deposited on (1 0 0) MgO and (0 1 2) $LaAlO_3$

| Substrate | Seed layer (Thickness nm) | Rs (B → 0) (mΩ, 77 K, 10 GHz) | △Rs/△B ($10^{-3}$ * mΩ/Oe) |
|---|---|---|---|
| MgO | No | 0.40 | 16.7 |
| MgO | $SrTiO_3$ (5) | 0.28 | 1.6 |
| MgO | $Ba_{0.15}Sr_{0.85}TiO_3$ (5) | 0.46 | 79.8 |
| MgO | $Ce_{0.78}La_{0.22}O_{1.89}$ (5) | >1 | — |
| MgO | $SrTiO_3/Ce_{0.78}La_{0.22}O_{1.89}$ (5/5) | 0.38 | 31.2 |
| MgO | $SrTiO_3/Ce_{0.78}La_{0.22}O_{1.89}$ (5/250) | 0.32 | 19 |
| $LaAlO_3$ | No | 0.26 | 9.0 |
| $LaAlO_3$ | $SrTiO_3$ (5) | > 1 | — |
| $LaAlO_3$ | $Ce_{0.78}La_{0.22}O_{1.89}$ (250) | 0.29 | 3.8 |

oxide layer but $SrTiO_3$ induces low surface resistance associated to low field dependency. Furthermore, this effect which is not observed using $LaAlO_3$ substrate could be specific to the MgO-$SrTiO_3$ system. However, it must be noticed that a thick $Ce_{0.78}La_{0.22}O_{1.89}$ buffer layer deposited on $LaAlO_3$ also reduces markedly by more than a factor 2 the field dependency of the surface resistance.

The resistive transition temperature is also increased by the deposition of the $SrTiO_3$ seed layer; it is between 91 and 92 K as for the films on $LaAlO_3$, whereas it is around 89 K for the best films deposited on bare MgO. On the other hand no significant change is observed in minimum yields of channeled Rutherford backscattering spectra, the $\chi_{min}$

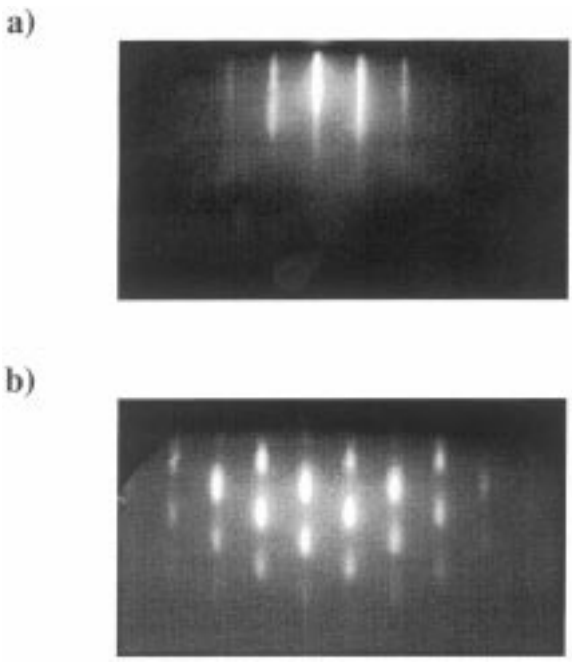


*Fig. 3.* RHEED patterns recorded along the (1 0 0) azimuth at the end of the growth of a 250 nm thick $Ce_{0.69}La_{0.31}O_{1.845}$ (a = 0.388 nm) layer grown on (1 0 0) $SrTiO_3$ (a) and (1 0 0) MgO (b).

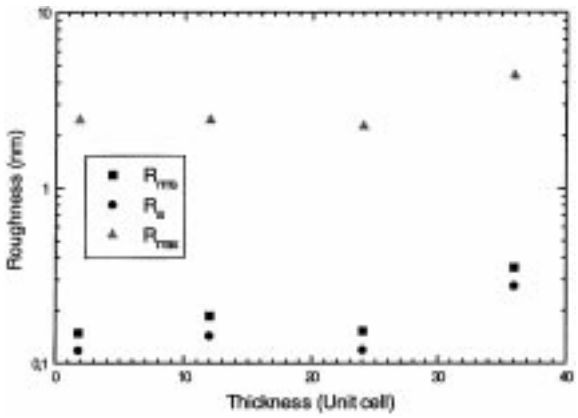


*Fig. 4.* AFM roughnesses over 5 $\mu$m recorded after the deposition of 6, 12, 24 and 36 $SrTiO_3$ unit cells on (1 0 0) MgO.

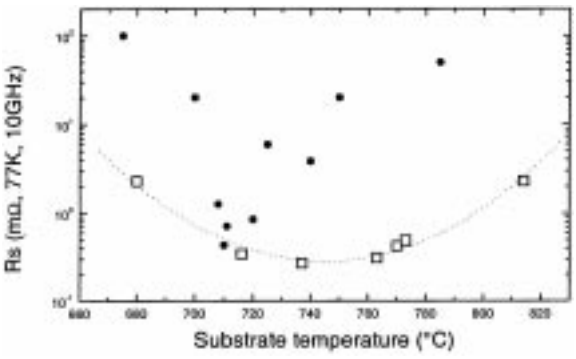


*Fig. 5.* Surface resistance (10 GHz, 77 K) of the YBCO layer as a function of the growth temperature (open square: YBCO/$SrTiO_3$/MgO, solid circle: YBCO/MgO).

values recorded on Ba signals at the surface being lower than 8%, for samples grown either on MgO, $LaAlO_3$ or $SrTiO_3$ buffered MgO.

X-ray diffraction has been used to determine the in-plane orientation of the YBCO layer on $SrTiO_3$ buffered MgO substrates by the Φ-scan of the (1 0 2) and (0 1 2) lines from films grown at the same temperature (740°C). As shown in Fig. 7, for bare MgO the prominent orientation is YBCO [1 1 0]// MgO [1 0 0] associated with a slight contribution of YBCO [1 0 0] // MgO [1 0 0], whereas the YBCO film on $SrTiO_3$ buffered MgO is mainly oriented with YBCO [1 0 0] // MgO [1 0 0]. The seed layer induces the epitaxial growth with the [1 0 0] axis of YBCO

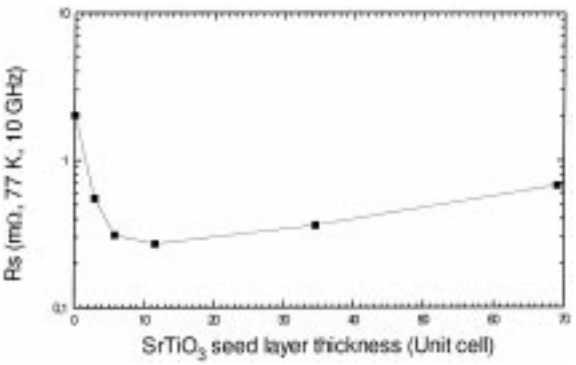


*Fig. 6.* Surface resistance (10 GHz, 77 K) of the 400 nm thick YBCO layer deposited at 740°C as a function of the thickness of the $SrTiO_3$ seed layer in elementary unit cell of $SrTiO_3$, i.e., 0.39 nm.

parallel to the one of the substrate, as it is observed in the low Rs YBCO layers deposited on MgO or $LaAlO_3$ [6,15,16]. Taking into account that this effect is not observed by using other buffer oxides ($CeO_2$, $Ce_{1-x}La_xO_2$, $Ba_xSr_{1-x}TiO_3$) or $SrTiO_3$ buffered $LaAlO_3$, it is assumed that the origin of this oriented growth is not linked to a mechanical effect of the buffer layer which reduces the mismatch between the MgO surface and the YBCO epitaxial film, but is the result of a chemical interaction between MgO and $SrTiO_3$ during the first stage of the epitaxial growth including the formation of an interfacial solid solution of spinel compounds from the MgO-SrO-$TiO_2$ system acting as a independent substrate surface [17–19].

## 4. Conclusion

In summary, we have shown that a buffer layer of $SrTiO_3$ deposited on (1 0 0) MgO with a thickness between 2 and 15 nm is sufficient to expand to more than 60°C the range of deposition temperatures leading to low microwave surface resistance of YBaCuO films for microwave applications [Rs(77 K, 10 GHz) $< 0.5$ mΩ]. The thickness of the buffer layer which is accurately controlled by *in-situ* RHEED measurements is of paramount importance to obtain the lowest Rs values in the subsequently deposited YBCO film. The Rs values are as good as those obtained on $LaAlO_3$ substrates with a slighly lower magnetic field dependency. The $SrTiO_3$ seed layer induces an oriented epitaxial growth with the (1 0 0) axis of YBCO parallel to that of MgO, which is assumed to result from an oriented growth and which is possibly promoted by the chemical interaction between MgO and $SrTiO_3$ during the first stage of the deposition.

## Acknowledgments

The authors are grateful to E. Jacquet and M. Mihet for their helpful contribution in the PLD growths and AFM measurements. They also thank J. Siejka (GPS, Université Denis Diderot) for the RBS analyses and J.C. Mage for valuable discussions.

## References

1. A. Porch, M.J. Lancaster, R.G. Humphreys, and N.G. Chew, *J. Alloys Comp.*, **195**, 563 (1993).

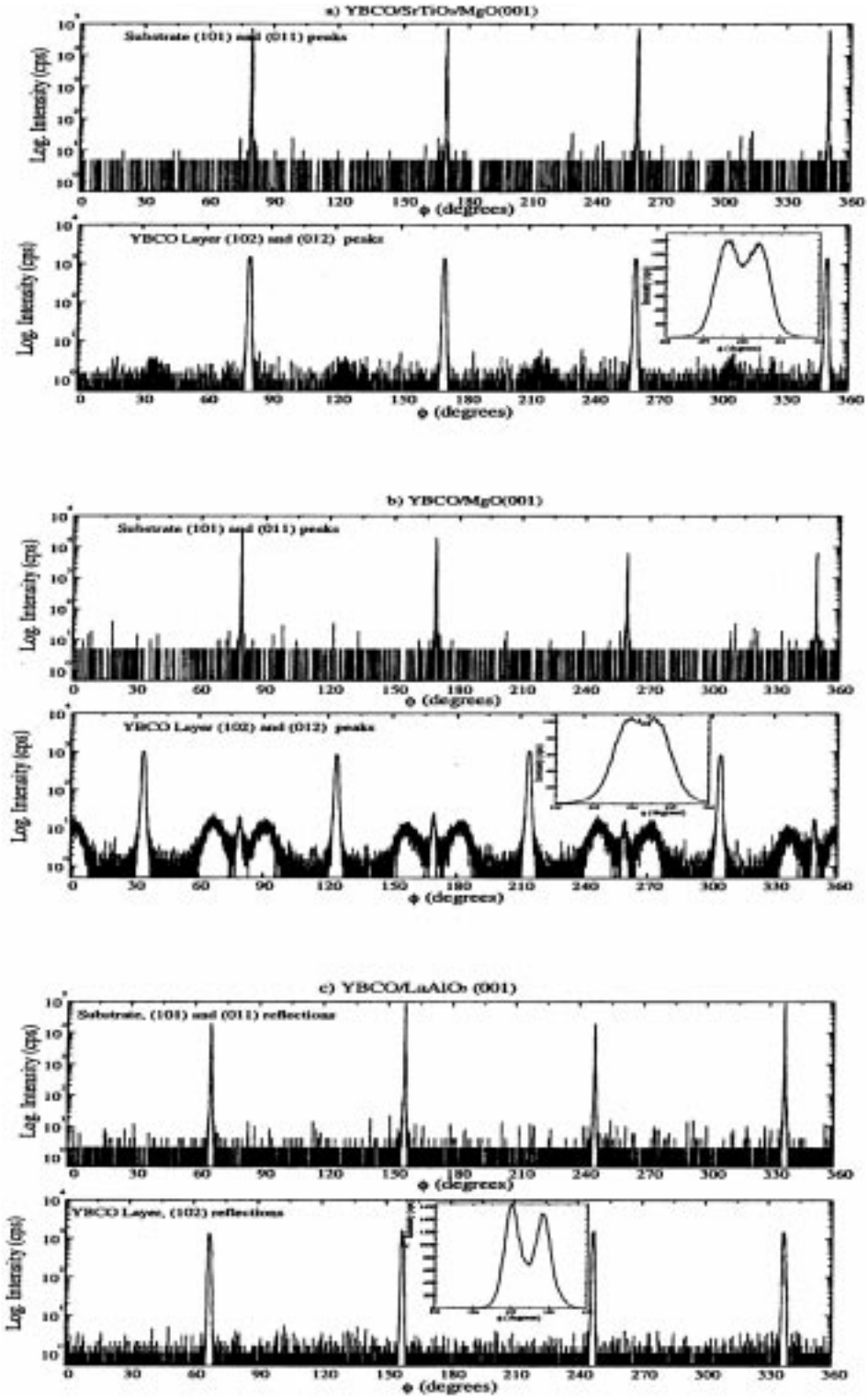


*Fig. 7.* XRD $\phi$-scan of a 400 nm thick YBCO layer: (a) on a 12 cell buffer layer of $SrTiO_3$ on (1 0 0) MgO substrate (Ts = 740°C, $PO_2$ = 40 Pa); (b) directly on (1 0 0) MgO (Ts = 740°C, $PO_2$ = 40 Pa); (c) on (0 1 2) $LaAlO_3$ (Ts = 780°C, $PO_2$ = 40 Pa).

2. S. Hensen, M. Lenkens, M. Getta, G. Müller, B. Avenhaus, A. Porch, and M.J. Lancaster, EUCAS'95, *Institute of Physics Conference Series*, **148**, 1127 (1995).
3. S.S. Ladermann, R.C. Taber, R.D. Jacowitz, J.L. Moll, C.B. Eom, T.L. Hylton, A.F. Marshall, T.H. Geballe, and M.R. Beasley, *Phys. Rev. B*, **43**, 2922 (1991).
4. A. Zaitsev, R. Würdenweber, G. Ockenfuss, C. Zuccaro, N. Klein, and T.B. Samoilova *6th International Superconductive Electronics Conf. (1997)* (Berlin, Germany).
5. D.W. Face, C. Wilker, J.J. Kingston, Z.Y. Shen, F.M. Pellicone, R.J. Small, S.P. McKenna, S. Sun, and P.J. Martin, *IEEE Trans. Appl. Supercond.*, **7**, 1283 (1997).
6. Y. Lemaître, D. Mansart, B. Marcilhac, J. Garcia-Lopez, J. Siejka, and J.C. Mage, *J. Alloys Comp.*, **251**, 166 (1997).
7. C. Prouteau, J.F. Hamet, B. Mercey, M. Hervieu, B. Raveau, D. Robbes, L. Coudrier, and G. Ben, *Physica C*, **248**, 108 (1995).
8. X.T. Cui, Q.Y. Chen, W.K. Chu, and Y.X. Guo, *Appl. Phys. Lett.* (private communication, to be published).
9. M.R. Rao, *Appl. Phys. Lett.*, **69**, 1957 (1996).
10. J.P. Contour, C. Couvert, O. Durand, Y. Lemaître, R. Lyonnet, and B. Marcilhac, *Eur. Phys. J. A.P.*, **5**, 3 (1998).
11. Y. Lemaître, L.M. Mercandalli, B. Dessertenne, D. Mansart, B. Marcilhac, and J.C. Mage, *Physica C*, **235–240**, 643 (1994).
12. J.C. Mage and J. Dieumegard, *AGARD Conf. Proceedings*, **481**, 104 (1990).
13. K. Bouzehouanne, J.P. Contour, and D. Ravelosona, *Le Vide*, **283**, 15 (1997).
14. A. Defossez, J.P. Contour, A. Abert, and P. Ziemann, *Z. Physik. B*, **100** (1996) 185.
15. X. Castel, M. Guilloux-Viry, A. Perrin, C. Le Paven-Tivet, and J. Debuigne, *Physica C*, **255**, 281 (1995).
16. C. Zuccaro, N. Klein, A.G. Zaitzev, R. Würdenweber, Y. Lemaître, and J.C. Mage, EUCAS'97, *Institute of Physics Conference Series*, **158**, 295 (1997).
17. *Gmelins Handbuch der anorganischen Chemie, System Nummer 41: Titan*, (Verlag-Chemie, Weinheim De, 1951), pp. 433–460.
18. H. Haefke, H.P. Lang, R. Sum, H.J. Güntherodt, L. Berthold, and D. Hesse, *Appl. Phys. Lett.*, **61**, 2359 (1992).
19. D. Hesse and H. Bethge, *J. Cryst. Growth*, **52**, 875 (1981).